

Amplifier-Based Active Antenna Oscillator Design at 0.9-1.8 GHz

I. Waldron*, A. Ahmed, and S. Makarov

ECE Dept., Worcester Polytechnic Institute, 100 Institute Rd., Worcester, MA 01609

iwaldron@wpi.edu

Abstract — The design of a stable narrowband active antenna oscillator at 0.9-1.8 GHz is reported. Novel use of a MMIC RF amplifier as the active device with two coupled patch resonators is presented. The design is based on EM-simulated antenna scattering parameters and manufacturer device measurements; this technique is confirmed by measurement of physical prototypes. Frequency tuning by varying the geometry or the supply voltage is observed and quantified.

Index Terms — Active antennas, microstrip antennas, microwave amplifiers, oscillators, scattering parameters.

I. INTRODUCTION

Active integrated antennas incorporate the local oscillator (LO) and in some cases a mixer using the patch antenna cavity as the LO resonating element. Thereby, the size, weight, and cost of a wireless system may be reduced. Several techniques for active oscillator design have been reported. These include the Gunn diode negative-resistance oscillator [1], the FET feedback oscillator [2], the FET oscillator with mixer diode [3], and the tunnel diode negative-resistance oscillator [4]. Chang *et al.* recently provided a review of active antenna research [5]. However, there are no reports of the use of RF amplifier MMICs in the design of active patch antenna oscillators. In this paper we discuss the design, construction, and measurement of a stable narrowband dual-patch active antenna oscillator at 0.9-1.8 GHz based on the Mini-Circuits ERA-2SM RF amplifier.

II. ACTIVE DEVICE AND ANTENNA SETUP

Mini-Circuits ERA-2SM RF amplifier was selected as the active device for the antenna. This is a broadband, DC-6 GHz low-cost amplifier that provides 15.8 dB gain at 1 GHz. The amplifier is characterized as a two-port network using scattering parameters provided by Mini-Circuits. The antenna concept is based on a symmetric pair of rectangular ($\sim\lambda/2$) patches with corner cutouts for integration with an active device. The antenna geometry is shown in Fig. 1. The active device is to be connected between the two small rectangles marked “Port1” and “Port2;” these two ports are the feed points of the antenna.

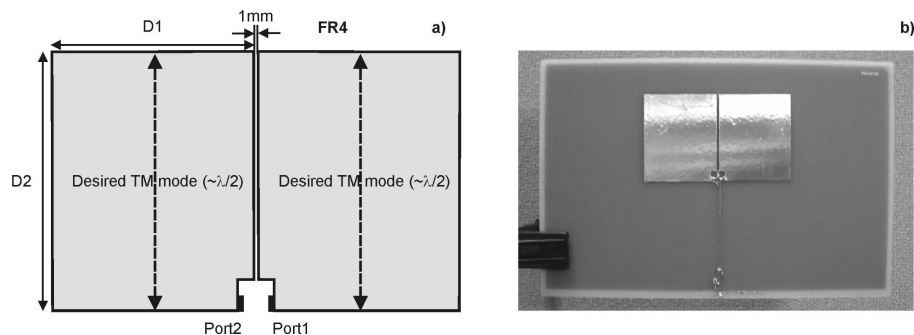


Fig. 1. a) - Antenna geometry, b) – typical oscillator setup.

Two patches form two coupled microstrip resonators. The coupling is due to a slot of a fixed width of 1mm. The desired mode for both patches is the (lowest) TM mode in the vertical direction (see Fig. 1a). This mode provides highest power output and easily controllable resonant frequency. The active device acts as a voltage amplifier from Port2

to Port1; this is due to the charge distribution of two coupled TM modes, which specifies maximum voltage difference at the patch edges along the gap. Additionally, using two patches provides the DC isolation that is required by the amplifier.

We used Ansoft Designer to simulate the scattering parameters of this two-port device. The oscillator circuit is constructed by inserting the active device between Port1 and Port2. The design of the oscillator follows from the Barkhausen criterion [6]. The antenna acts as a frequency selective feedback network for the amplifier. The oscillation condition implies zero denominator of the closed-loop transfer function:

$$1 - H_{\text{amp}}(\omega)H_{\text{ant}}(\omega) = 0 \quad (1)$$

The oscillation condition (1) is to be expressed in terms of S -parameters of both the antenna and the amplifier. One has

$$H_{\text{amp}}(\omega)H_{\text{ant}}(\omega) = [S_{\text{loop}}]_{21} \quad (2)$$

where $[S_{\text{loop}}]$ is the scattering matrix of the open loop. This matrix is obtained from the scattering matrices of the active device and the antenna by converting them to chain scattering matrices [7] and then multiplying:

$$[S_{\text{amp}}] \Rightarrow [T_{\text{amp}}], [S_{\text{ant}}] \Rightarrow [T_{\text{ant}}], [T_{\text{loop}}] = [T_{\text{amp}}][T_{\text{ant}}], [T_{\text{loop}}] \Rightarrow [S_{\text{loop}}] \quad (3)$$

Given the scattering parameters of the loop, the steady-state oscillation condition is

$$|[S_{\text{loop}}]_{21}| = 1, \angle([S_{\text{loop}}]_{21}) = 0^\circ \quad (4)$$

In order to ensure oscillation startup, the magnitude of S_{21} at the zero-phase crossing must be greater than unity. From the scattering parameters of the oscillator loop, we may also compute the impedance across the terminals of the open loop. This corresponds to the negative resistance technique ([5], [8]). The impedance matrix $[Z_{\text{loop}}]$ may be calculated from the scattering matrix $[S_{\text{loop}}]$, and the equivalent circuit impedance is given by:

$$Z_{\text{eq}} = [Z_{\text{loop}}]_{11} + [Z_{\text{loop}}]_{22} - [Z_{\text{loop}}]_{12} - [Z_{\text{loop}}]_{21} \quad (5)$$

The oscillation startup conditions for the negative resistance technique are that the equivalent loop resistance is negative where the equivalent reactance is close to zero.

III. GEOMETRY DEPENDENT OSCILLATION CONDITIONS

Theory simulations for the oscillation startup conditions were performed in a wide range of two patch parameters: width D_1 and height D_2 . Further, the corresponding antennas were built and the frequency of oscillation and the radiated power were measured using an Agilent E4445A spectrum analyzer. Prototype oscillators were built on 62 mil thick FR-4 substrate to confirm our design. The PCB was constructed with only the traces necessary for mounting and biasing the amplifier; the antenna element was added by applying appropriately cut and shaped adhesive copper tape to the board. This provided maximum flexibility in the testing of the antenna oscillator. The ERA-2SM requires a simple biasing setup consisting of a 100 Ω current-limiting resistor and 680 nH RF-blocking inductor. The nominal supply voltage is 7.5 V. Additionally, a 1000 pF capacitor was placed across the power supply. A linearly-polarized UWB antenna was used on the receiver side.

It has been found, both numerically and experimentally, that the oscillation conditions on the D_1, D_2 plane fall into the three regions shown in Fig. 2a. In region I, there is stable

high-power oscillation with good polarization isolation (~ 20 dB). The vertical polarization is dominant. In region III, the oscillator generates lower power (~ 25 dB less), and polarization isolation is not well developed. This indicates weak coupling between the patches and simultaneous excitation of two perpendicular patch modes. In region II, the oscillation power may be higher but the polarization is either dual or reversed. Hence, the horizontal TM mode may simultaneously be excited in this region. Fig. 2b and c show a typical example of region transition for $D_1 = 34$ mm.

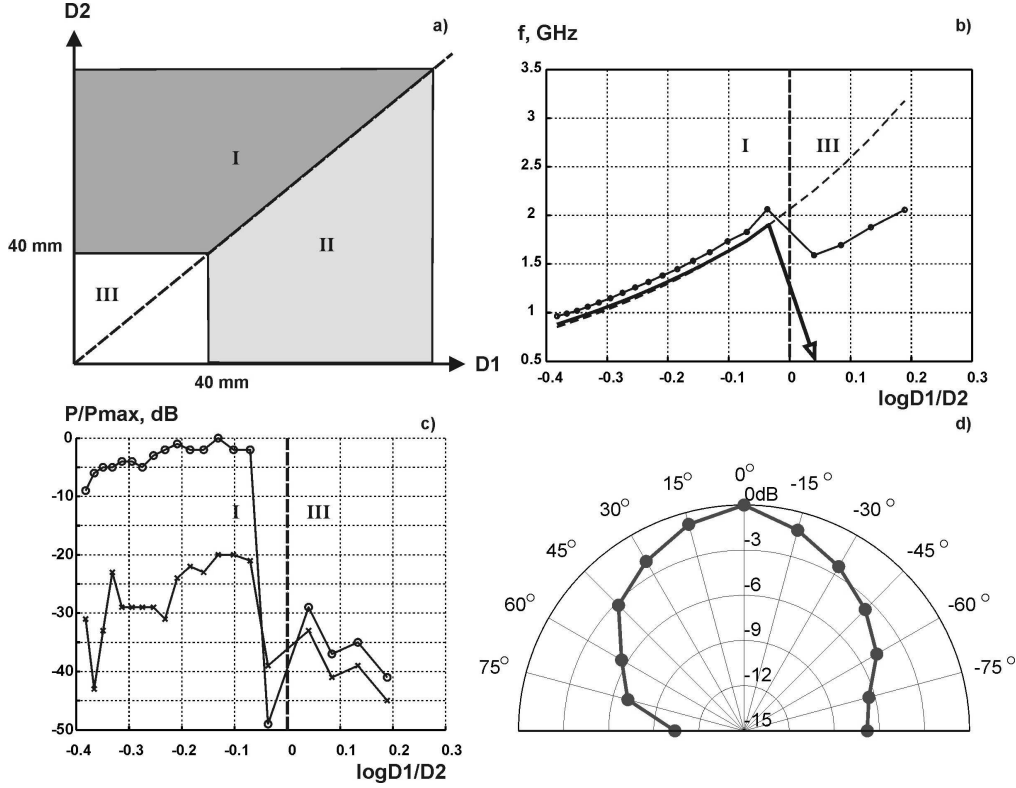


Fig. 2. a) Three regions of operation of the active antenna; b) resonant frequency at $D_1 = 34$ mm and D_2 varying. Thick curve – Ansoft Designer simulation; circles – experiment; dashed curve – $c/(2D_2\epsilon_r^{1/2})$ approximation. Arrow on the simulation plot indicates no oscillation (no negative resistance) after the break point; c) peak signal power for two polarizations for the Fig. 2b antenna; d) relative received power in E -plane at 1.27 GHz.

IV. ACTIVE ANTENNA OPERATION IN REGION I

A prototype in region I ($D_1 = 48.5$ mm; $D_2 = 59$ mm) was selected for additional testing. As shown in Fig. 3a, the center frequency of oscillation was approximately 1.2615 GHz. The short-term frequency stability was quite good; the center frequency remained within a range of ± 100 kHz of the initial value over a period of 20 minutes. Long-term stability was not investigated. The oscillator exhibited a 99 % power occupied bandwidth of 10.2 kHz. The bandwidth of the oscillations, less than 0.001 percent of the center frequency, is extremely narrow. This result is comparable to other reported active antenna oscillators [9]-[11]. The bandwidth measurement is also shown in Fig. 3a; of note are two side lobes at ± 20 kHz and ± 80 kHz from the carrier. We measured the phase noise performance of the oscillator to investigate these side lobes. The phase noise measurement exhibited significant peaks of -20 dBc/Hz at 15 and 20 kHz offset from the carrier, and -90 dBc/Hz at 80 and 100 kHz offset from the carrier. At 1 MHz offset from the carrier, the phase noise is -120 dBc/Hz. The oscillator exhibited injection locking to

signals within ~ 100 kHz on either side of the free-running frequency and maintained lock within ~ 200 kHz on either side of the free-running frequency. The free-running frequency exhibits near-linear dependence on the DC supply voltage of the amplifier over a small tuning range of 6.5 V to 8.1 V, as shown in Fig. 3b. The tuning sensitivity is approximately 1.13 MHz per volt.

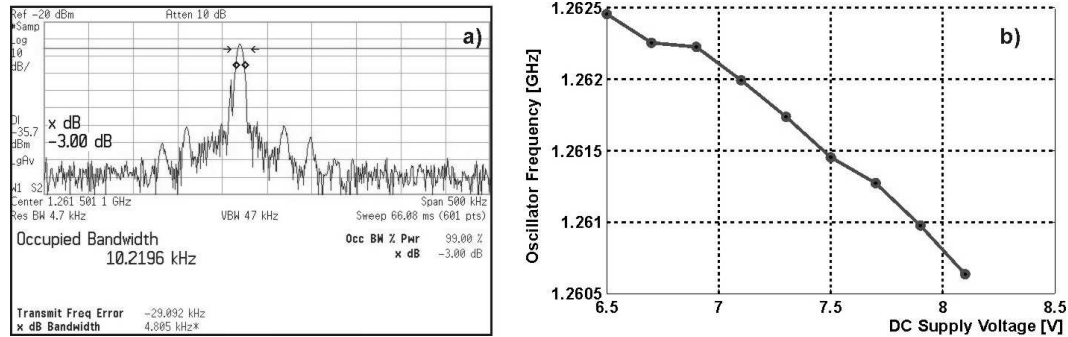


Fig. 3. a) Oscillator spectrum and bandwidth; b) oscillation frequency vs. DC supply voltage.

V. CONCLUSION

A geometric design of an active antenna oscillator based on a MMIC RF amplifier at 0.9-1.8 GHz is presented. The measured oscillation frequencies differ only slightly from predicted startup values. The oscillation bandwidth of the antenna is very narrow, and phase noise is fairly low. The oscillator exhibits good short-term stability; its free-running frequency varied within a range of ± 100 kHz. Dependence of the center operating frequency on DC supply voltage of the amplifier is observed and quantified.

Our design method correctly predicts oscillations up to approximately 1.8 GHz. Above this frequency, reduced coupling between the patches usually causes oscillations to cease. In order to generate higher frequency oscillations, we will investigate methods of increasing the coupling between patches.

REFERENCES

- [1] C. M. Montiel, L. Fan, and K. Chang, "A novel active antenna with self-mixing and wideband varactors-tuning capabilities for communication and vehicle identification application." *IEEE Trans. Microwave Theory Techniques*, pp. 2421-2430, Dec. 1996.
- [2] W.K. Leverich, X.-D. Wu, and K. Chang, "New FET active notch antenna." *IEE Electronics Letters*, vol. 28, issue 24, pp. 2239-2240. Nov. 19, 1992.
- [3] R. Flynt, F. Lu, J. Navarro, and K. Chang, "Low cost and compact active integrated antenna transceiver for system applications." *Microwave Symposium Digest, 1995, IEEE MTT International Sym.*, vol. 2, pp. 953-956, May 1995.
- [4] K. Liu, S.M. El-Ghazaly, M.R. Deshpande, V. Nair, N. El-Zein, and H. Goronkin, "Active antennas incorporating tunnel diodes-large signal model approach." *IEEE Microwave and Wireless Components Letters*, vol. 11, issue 8, pp. 331-333. Aug. 2001.
- [5] K. Chang, R. York, P. Hall, and T. Itoh, "Active integrated antennas." *IEEE Transactions on Microwave Theory and Techniques*, vol. 50, no. 3, pp. 937-944. Mar. 2002.
- [6] D. Pozar, *Microwave Engineering*, third edition, p. 578. John Wiley & Sons, Inc. 2005.
- [7] R. Ludwig and P. Bretchko, *RF Circuit Design: Theory and Applications*, pp. 175-176. Prentice-Hall, Inc. Upper Saddle River, New Jersey, USA. 2000.
- [8] S.D. MacPherson, "High Frequency Oscillator Design Using the Technique of Negative Resistance." *Proceedings of 1999 IEEE AFRICON*, pp. 1111-1114. Sept. 28 – Oct. 1, 1999.
- [9] J. Bartolic, D. Bonefacic, and Z. Sipus, "Modified rectangular patches for self-oscillating active-antenna applications." *IEEE Antennas and Propagation Magazine*, vol. 38, issue 4, pp. 13-21. Aug. 1996.
- [10] J.W. Andrews and P.S. Hall, "Oscillator stability and phase noise reduction in phase locked active microstrip patch antenna." *IEE Electronics Letters*, vol. 34, no. 9, pp. 833-835. Apr. 30, 1998.
- [11] Y. Yu-On, L. Man-Lung, and N. Tsz-Bun, "Active Integrated Radiator for Microwave Sensing System." *Proceedings of the 1991 Int. Conference on Circuits and Systems*, vol. 2, pp. 952-955. 16-17 June, 1991.